Zeolites for CO_2-CO-O_2 separation to obtain CO_2-neutral fuels

Julio Perez-Carbajo [a], *Ismael Matito-Martos* [a], *Salvador R. G. Balestra* [a], *Mihalis N. Tsampas* [b], *Mauritius C. M. van de Sanden* [b,d], *José A. Delgado* [c], *V. Ismael Águeda* [c], *Patrick J. Merkling* [a] *and Sofia Calero* [a,b,d,*]

[a] Department of Physical, Chemical, and Natural Systems, Universidad Pablo de Olavide, Ctra. Utrera km 1, 41013 Seville, Spain

[b] DIFFER, Dutch Institute For Fundamental Energy Research, De Zaale 20, 5612 AJ Eindhoven, The Netherlands

[c] Department of Chemical Engineering, Universidad Complutense de Madrid, 28040, Madrid, Spain

[d] Technische Universiteit Eindhoven, 5600 MB Eindhoven, The Netherlands

KEYWORDS

CO_2-neutral fuel, zeolites, gas separation, CO_2, CO, O_2.

ABSTRACT

Carbon dioxide release has become an important global issue due to the significant and continuous rise in atmospheric CO_2 concentrations and depletion of carbon-based energy resources. Plasmolysis is a very energy efficient process for reintroducing CO_2 into energy and chemical cycles, by converting CO_2 into CO and O_2 utilizing renewable electricity. The bottleneck of the process is that CO remains mixed with O_2 and residual CO_2. Therefore, efficient gas separation and recuperation is essential for obtaining pure CO, which via water gas shift and Fischer-Tropsch reactions, can lead to the production of CO_2 neutral fuels. The idea behind this work is to provide a separation mechanism based on zeolites to optimize the separation of carbon dioxide, carbon monoxide and oxygen at mild operational conditions. To achieve this goal, we performed a thorough screening of available zeolites based on topology and adsorptive properties using molecular simulation and Ideal Adsorption Solution Theory. FAU, BRE and MTW are identified as suitable topologies for these separation processes. FAU can be used for the separation of carbon dioxide from carbon monoxide and oxygen and BRE or MTW for the separation of carbon monoxide from oxygen. These results are reinforced by pressure swing adsorption simulations at room temperature combining adsorption columns with pure silica FAU zeolite and zeolite BRE at a Si:Al ratio of 3. These zeolites have the added advantage of being commercially available.

1. INTRODUCTION

Reducing greenhouse gas (GHG) emissions has been identified as one of the principal keys to mitigate climate change. It was already pointed out two decades ago in the Kyoto Protocol (1997) and reinforced by the Copenhagen Accord (2009) and the 21st Conference of the Parties

agreements, also known as the Paris Climate Change Conference (2015). Although the increasing rate of pollutant emissions has been slowed down over the last years, total carbon emissions keep rising, as well as carbon-based fuel demand.[1, 2] Thus, finding alternatives to overcome the fossil fuel dependence while at the same time decreasing the GHG emissions is a goal behind both research and industrial efforts. The search for new clean-energy technologies is driven by the challenge of reducing these gas emissions and the desire to make industrial processes environmentally sustainable.

A promising solution is the large-scale replacement of fossil fuel by renewable energy sources.[3-6] Wind or photovoltaics integration into energy-intensive industries is presently hampered by their intermittency in conjunction with the absence of useful storage solutions. Additionally, the direct introduction of sustainable energy into, e.g., the value chain of chemical industry remains challenging: Heat is the desired form of energy, whereas renewables are frequently harvested in the form of electricity. Therefore technologies that can convert renewable electricity into storable chemical fuels have attracted tremendous interest.[3-6]

Carbon dioxide is often considered as the key molecule in many strategies to replace conventional energy sources by renewable ones. Although the dissociation of CO_2 is a strongly endothermic process, a sustainable production of CO or syngas, $CO + H_2$ (via the water gas shift reaction: $CO + H_2O \rightarrow CO_2 + H_2$) would be an elegant route to implement renewable energy into the chemical production chain while adding value to the waste gas CO_2. Synthesis gas is used in the petroleum industry for long-chain liquid hydrocarbons via the Fischer-Tropsch process.[3]

Carbon dioxide splitting mechanisms are energy-costly processes per se, however non-thermal plasma-assisted dissociation has been proved to be able to reach energy efficiency of 80%.[4-6] These electrical discharges are characterized by non-equilibrium conditions under which

electrons, ions, and neutral species have different translational and — in the case of molecules — internal energies. The corresponding energy distribution functions may be described by separate temperatures. Therefore, non-thermal plasmas with unequal electron, gas, and vibrational temperatures provide an entirely different environment for chemical reactions than known from conventional processing under thermal equilibrium. In the case of CO_2 dissociation (to CO and O_2) or CO_2 plasmolysis under non-thermal conditions, the vibrational excitation of CO_2 molecules in a plasma process provides the highest energy efficient route for its dissociation. In order to maintain high efficiencies for CO_2 plasmolysis, low CO_2 conversion should be implemented which results in the production of a CO_2, CO and O_2 mixture. Therefore an extra separation step for obtaining pure CO is necessary before the utilization for both water gas shift and syngas-to-fuel processes, as depicted in the diagram of Figure 1.

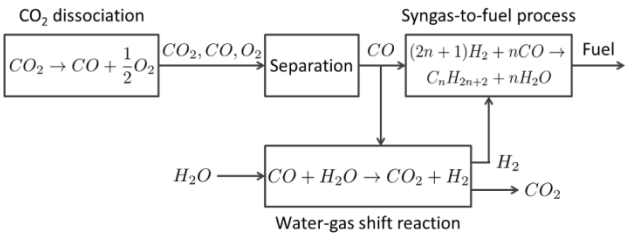

Figure 1. Diagram of the CO_2-neutral production of fuel.

Nanoporous materials are commonly used for gas flow sieving. In particular, zeolites have been previously proposed as materials that can perform highly selective separations. This is one of the reasons for their wide use in industry. Zeolites are well known porous crystalline structures made of TO_4 tetrahedra, where the tetravalent central atom T is usually a silicon atom. These basic blocks form different building units which allow zeolites to adopt a large number of topologies, with a wide range of molecular-sized pores and high surface areas. Molecular simulation is a useful tool for finding suitable materials for gas separation, considering many factors and conditions. Despite the fact that multi-component simulations in complex systems

require significant amounts of time and resources, the evolution of computational algorithms, theoretical approaches, and hardware technology make them affordable nowadays. Additionally, molecular simulations offer some advantages over experiments, providing complete control over the system, producing information at a molecular level, and allowing screenings which would be unfeasible using other approaches. In this sense, several works of the literature validate simulation procedures in zeolite screenings.[7-13] Essentially, screening can be tackled in one of two ways. The first one is dealing with reduced, preselected sets of porous materials (up to typically 20) and performing a specific study on the separation of a particular mixture based on sorption and/or diffusion criteria.[7-9] The second one is to perform coarse-grained characterizations of large structure databases to aid further aimed research, but limiting the study to calculations derived from heat of adsorption results.[10, 11] Although some recent works start to overcome these computational restrictions,[12, 13] widespread detailed studies remain challenging.

This work focuses on finding an effective separation scheme to capture carbon dioxide and recover carbon monoxide from a gas mixture made of CO_2 (85%), CO (10%) and O_2 (5%). This composition is typical of carbon dioxide splitting as reported in Fridman [6], Van Rooij *et al.*[4], and Bongers *et al.*[14] Pure component adsorption isotherms were calculated for the three gases in most of the zeolite topologies reported in the IZA database.[15] A first approximation to adsorption isotherms for the mixture were obtained applying Ideal Adsorption Solution Theory (IAST).[16] We also simulated adsorption isotherms of binary and ternary mixtures in selected zeolites. Simulations of pressure swing adsorption processes were performed to confirm the feasibility of the separation scheme suggested.

2. METHODOLOGY

Adsorption isotherms were obtained using Monte Carlo simulation in the Grand Canonical ensemble (μVT). This ensemble fixes the average value of the chemical potential, volume, and temperature. Due to the nature of our systems, the chemical potential of a gas can be directly related with the fugacity, and thereby with the pressure through the fugacity coefficient, using the Peng-Robinson equation of state. RASPA software[17] was used to carry out all simulations. Temperature was set to 298 K and the pressure values used for the adsorption isotherms were selected in the range of 10^0-10^{12} Pa, depending on the zeolite.

The gas molecules are described by rigid three-site models. Each site is considered as an interacting center with a point charge and effective Lennard-Jones potentials. The parameters used are compiled in Table 1.

Table 1. Lennard-Jones parameters and point charges used for the adsorbates.

	ε/k_B [K]	σ [Å]	q [e^-]
C_{CO_2}	29.993	2.745	+ 0.6512
O_{CO_2}	85.671	3.017	– 0.3256
C_{CO}	16.141	3.658	– 0.2424
O_{CO}	98.014	2.979	– 0.2744
D_{CO}	-	-	+ 0.5168
O_{O_2}	53.023	3.045	– 0.112
D_{O_2}	-	-	+ 0.224

While each site of the carbon dioxide molecule corresponds to an atom center, for carbon monoxide and oxygen a central dummy pseudo-atom (D_{CO} and D_{O_2}, respectively) are defined to reproduce their first non-zero electrostatic moment. These dummies are therefore interacting centers with non-zero point charges, but their Lennard-Jones parameters and mass are set to zero.

The point charges and Lennard-Jones parameters for carbon dioxide are taken from Garcia-Sanchez *et al.*[18], and those for carbon monoxide and oxygen from Martin-Calvo *et al.*[19, 20]

Zeolites are considered rigid and, for the initial screening, we focused only on pure silica structures. Among all the zeolite topologies contained in the IZA database,[15] we selected a subset of 174 structures, avoiding the structures defined as 0-dimensional and also the structures containing OH groups. The point charges for the atoms of the framework ($q_{Si} = +0.786\ e^-$ and $q_O = -0.393\ e^-$) are also taken from Garcia-Sanchez *et al.*[18] Further simulations in selected zeolites were performed considering not only silicon atoms in their structures, but also aluminum atoms in the lattices. Given that Al atoms and oxygen atoms bridging silicon and aluminum atoms ($q_{Al} = +0.4859\ e^-$, $q_{O_a} = -0.4138\ e^-$)[18] differ from Si atoms and oxygen atoms linking two Si atoms, non-framework cations have to be introduced to compensate the net charge. One sodium cation, with charge $q_{Na} = +0.3834\ e^-$,[18] is introduced for each T central silicon atom replaced by an aluminum atom.

Adsorbate-adsorbate and adsorbate-adsorbent atomic interactions are described by Lennard-Jones and Coulombic potentials. Lennard-Jones potentials are cut and shifted to zero at a cutoff radius of 12 Å. Coulombic interactions were calculated using Ewald summation. Interactions between framework atoms are not taken into account because their positions are kept fixed. Lennard-Jones interactions of guest molecules with framework silicon atoms are neglected, since their dispersive forces with the oxygen atoms prevail. Cross interactions are collected in Table 2. They imply that the carbon monoxide model leads to strong interactions with sodium cations to account for the significant quadrupole moment of this molecule. Other interactions not specified in the table are calculated using Lorentz-Berthelot rules. Additional Lennard-Jones parameters for cross terms between adsorbate molecules and sodium cations are also summarized in Table 2.

In terms of dispersion forces, O_a atoms are assumed to behave identically to Si-O-Si oxygen atoms. All the forcefields used in this work are parameterized to reproduce adsorption properties in zeolites and have been extensively validated. [19-21]

Table 2. Cross interaction Lennard-Jones parameters.

	ε/k_B $[K]$	σ [Å]
$C_{CO_2} - O_{zeo}$ [18]	37.595	3.511
$O_{CO_2} - O_{zeo}$ [18]	78.98	3.237
$C_{CO} - O_{zeo}$ [18]	40.109	3.379
$O_{CO} - O_{zeo}$ [18]	98.839	3.057
$O_{O_2} - O_{zeo}$ [20]	65.189	3.129
$C_{CO} - Na$ [21]	369.343	2.332
$O_{CO} - Na$ [21]	579.793	2.212
$O_{O_2} - Na$ [21]	241.284	2.06

Ideal Adsorption Solution Theory (IAST)[16] is applied to predict mixture behavior from modeling pure compound adsorption using the Dual-Site Langmuir equation[22] in Gaiast software.[23] We calculated adsorption for the $CO_2/CO/O_2$ ternary mixture and for the remaining CO/O_2 binary mixture once the molecules of carbon dioxide are removed. The preferential adsorption of one gas over the others is identified by the adsorption selectivity. This property (S_{ij}) is defined as the ratio between the adsorbed amount (x_i) and the molar fraction (y_i) of component *i* over the adsorbed amount (x_j) and the molar fraction (y_j) of component *j*.

Pressure swing adsorption (PSA) simulations have been carried out with PSASIM software [24] in those structures selected to perform the desired separations. It has been assumed that the PSA processes are adiabatic to resemble the usual conditions of industrial PSA cycles. It is also assumed that the adsorbent crystals are agglomerated in pellets, and that mass transfer between gas and adsorbent is controlled by macropore diffusion, neglecting intracrystalline resistance.[25]

3. RESULTS AND DISCUSSION

To design the separation process for the mixture composed of carbon dioxide (85%), carbon monoxide (10%) and oxygen (5%), we performed two independent screenings. The first screening was meant to identify the optimal structure for the separation of carbon dioxide from carbon monoxide and oxygen, as carbon dioxide is more strongly adsorbed in all structures, and a second screening to separate the two remaining gases. Figure 2 shows the adsorption selectivity of carbon dioxide over the second most adsorbed species, either carbon monoxide or oxygen, as a function of the specific surface area of the zeolites, and as a function of the effective pore diameter. A table containing the numerical values is also provided in the Supporting Information (Table S1). The adsorption selectivity is obtained from the adsorption isotherms of the ternary mixture, at operating conditions of 25 degrees Celsius (298 K) and 1-10 atmospheres (10^5-10^6 Pa). The surface area of the zeolites is calculated with the RASPA code by rolling an atom over the surface of the structure. The fraction of overlap with the structure is calculated from the points that are generated on a sphere around each atom of the framework. This fraction is multiplied by the area of the sphere, and the summation over all framework atoms provides the geometric surface area. The optimal structure for the separation sought should provide a large surface area and at the same time high selectivity for carbon dioxide over the other two components of the mixture. As seen in Figure 2, these two properties tend to be inversely related, since physisorption for small gases usually involves confinement.[26] A few structures stand out because they combine high selectivity, reasonable surface areas and additionally big pore diameters, which favor the mobility of the guest molecules: MRE and ATN zeolites have the largest selectivities for carbon dioxide but low specific surface area and moderate and very low pore diameter, respectively. Both of them are one-dimensional zeolites with non-interpenetrating

pores of 10-membered ring (10-MR) 5.6×5.6 $Å^2$ for MRE and 8-MR 4.0×4.0 $Å^2$ for ATN. Therefore the windows in these structures are far narrower compared with the opening in the FAU-type framework, which is almost 7.4 Å wide. The pores of FAU are also defined by 12-MR, leading into larger cavities of 12 Å in diameter. These cavities are surrounded by ten sodalite cages (truncated octahedra), that are connected on their hexagonal faces. The sodalite cages are inaccessible to the molecules of carbon dioxide, carbon monoxide and oxygen. On the other hand, RWY (also formed by 12-MR channels) is the zeolite with the largest pore diameter and high surface area, and therefore high storage capacity for carbon dioxide, but has relatively low separation selectivity. The structures of MRE, ATN, FAU and RWY are depicted in Figure S1 of the Supporting Information.

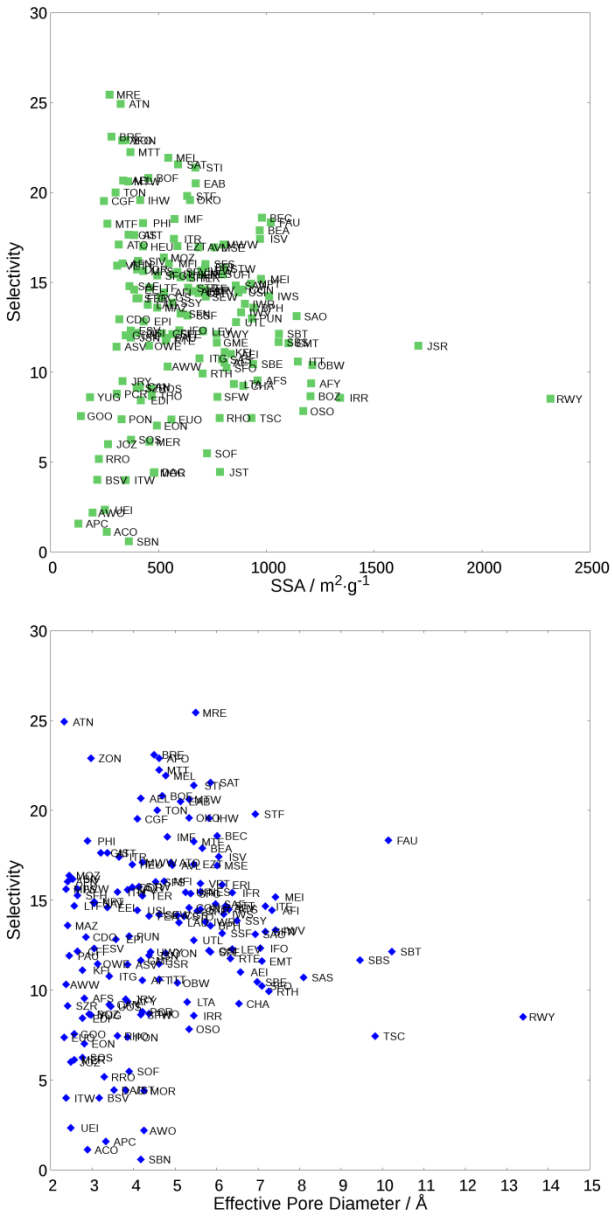

Figure 2. Maximum adsorption selectivity of carbon dioxide over the second most adsorbed species (carbon monoxide or oxygen) as a function of the specific surface area (top) and the effective pore diameter (bottom). Selectivity values were obtained at 10^5-10^6 Pa, from the adsorption isotherms of the ternary mixtures at 298 K obtained by applying IAST.

On the basis of Figure 2, we mentioned the importance of effective pore diameters, since they strongly affect molecular diffusion. The effective pore diameter is obtained from the analysis of

the pore size distribution (PSD) that we have calculated for each empty framework. It is defined as the smallest pore able to host a molecule of adsorbate having a kinetic radius larger than 2.298 Å, if the PSD peak associated to that pore represents at least 15% of the frequency of the most common pore. It should be large enough to enable diffusion but small enough for carbon dioxide adsorption. We also considered the selectivity related to the capacity of zeolites for capturing carbon dioxide. Figure S2 in the Supporting Information shows selectivity curves for the adsorbed loading of carbon dioxide corresponding to the range of pressures between 1 and 10 atm. The choice of high selectivity together with the relevant carbon dioxide uptake is necessary given that carbon dioxide is present in large excess in the considered mixtures. Otherwise it would be still present in substantial amounts after the carbon dioxide removal step. Therefore, based on Figure 2 and Figure S2b, zeolite FAU represents a compromise for this separation between selectivity for carbon dioxide of 17-18 with uptakes up to 5.2 mol/kg at the operating conditions (Figure S3 of the Supporting Information) and still relatively large specific surface area (1020.88 $m^2 \cdot g^{-1}$) and effective pore diameter (10.14 Å).

FAU can also be used to separate our ternary mixture at temperatures higher than 298 K. However, a temperature increase of 100 degrees also requires increasing the pressure by one order of magnitude to maintain the carbon dioxide capture but entails a notable decrease in the selectivity towards carbon dioxide (see Figure S4 of the Supporting Information). Similarly, a decrease in temperature of 100 degrees at constant pressure (10^5 and 10^6 Pa) increases the adsorption selectivity towards carbon dioxide by one order of magnitude (Figure 3).

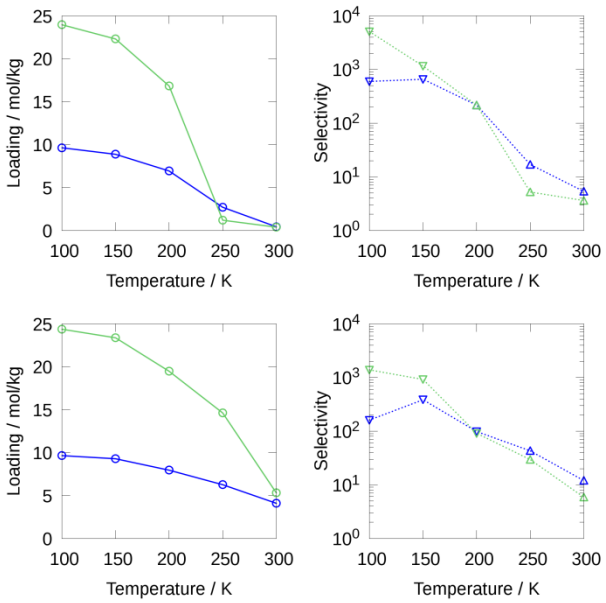

Figure 3. Adsorption of carbon dioxide (left) and adsorption selectivity in favor of carbon dioxide (right) in RWY (green) and FAU (blue) zeolites versus temperature. Both, adsorption loading and adsorption selectivity are taken from adsorption isotherms resulting from molecular simulation of the ternary mixtures at values of pressure of 10^5 (up) and 10^6 Pa (down). In all cases the adsorption selectivity depicted is the one obtained for the most unfavorable case between carbon dioxide over carbon monoxide (up-triangles) or oxygen (down-triangles).

The adsorption selectivity was also calculated for RWY under these operating conditions. We selected the zeolite with the largest effective pore to evaluate the trade-off between adsorption capacity and selectivity. It is interesting to note that this compromise is much lower at 10^6 Pa than at 10^5 Pa. Surprisingly enough, at 200 K and 10^6 Pa the adsorption selectivity in both zeolites is almost the same, whereas RWY doubles FAU in adsorption capacity. Unfortunately, at operating conditions of 300 K and 10^5-10^6 Pa, the selectivity in RWY is always lower than in FAU and so capturing significant traces of carbon monoxide. Although, based on the combination of capacity, selectivity, specific surface area and effective pore diameter, we rely

upon FAU for this separation, other structures such as BEA, BEC, ISV and GIS could also be candidates for it. Like FAU, the first three framework topologies have a three-dimensional large 12-MR pore system: both BEA and ISV are tetragonal structures with systems of 12-MR interconnected straight channels with cylindrical cavities, while BEC (tetragonal) and FAU (cubic) contains large cages connected by 12-MR windows. GIS also has a three-dimensional intersecting-channel pore system, but connected through 8-MR windows. The adsorption isotherms of the ternary mixture for these structures are collected in Figure S5 of the Supporting Information.

The mixture, after complete removal of carbon dioxide, is formed by CO (67%) and O_2 (33%). As mentioned above, the separation of these two components of the mixture is tricky because of their similarity in size, shape and polarity. We performed a screening based on the adsorption isotherms of the binary mixtures in all zeolites. The screening shows that none of these zeolites can separate completely the two components of the mixture at the operating conditions initially considered, i.e. 300 K and 10^5-10^6 Pa. Though the selectivity is very low, we found that under these conditions of temperature and pressure, zeolites such as AEI preferentially adsorbed oxygen over carbon monoxide, whereas the adsorption selectivity for zeolites such as BRE, THO and RTE is towards carbon monoxide (Figure S6 of the Supporting Information). In zeolites such as MTW, the increase in pressure once adsorption gets significant leads to reasonable values of adsorption selectivity, always in favor of molecular oxygen (Figure 4, left). However, for other zeolites such as BRE, the increase in pressure at a given temperature leads to an inversion of the selectivity (Figure 4, right). Hence, contrary to most structures, selectivity towards carbon monoxide decreases when pressure increases and at 10^8 Pa the preferential adsorption of the structure switches from carbon monoxide to oxygen. This is probably due to size entropy effects

since oxygen packs more efficiently than carbon dioxide in all structures at higher molecular loadings. The same effect is observed when decreasing the temperature to 100 K in the pressure range 10^5-10^6 Pa.

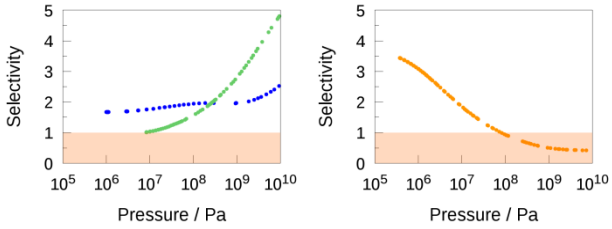

Figure 4. Left: Adsorption selectivity of oxygen over carbon monoxide as a function of pressure in MTW (green) and AEI (blue). Right: Adsorption selectivity of carbon monoxide over oxygen in BRE (orange). Note the inversion of preferential adsorption at 10^8 Pa. The adsorption selectivity is obtained from the binary adsorption isotherms of carbon monoxide (67%) and oxygen (33%) obtained by applying IAST.

In search of a structure with better separation performance at the initial operating conditions, we turned to aluminum containing MTW and BRE structures for which we performed additional simulations using sodium as non-framework cations. Firstly, we generated low-energy structures with 2 and 4 aluminum atoms per unit cell. To this end, the first silicon by aluminum substitution is determined randomly. The following sequential silicon by aluminum substitutions select those atoms whose average distance to existing aluminum atoms are maximized, provided the substitution observes Löwenstein's and Dempsey's rules, which forbids Al-O-Al linkages and minimizes the number of Al-O-Si-O-Al elements, respectively.[27, 28]

The adsorption isotherms for the binary mixtures in the two MTW structures containing cations lead to smaller values of selectivity compared to those obtained in the pure silica structures, even favoring carbon monoxide below 10^{10} Pa. In other words, the presence of cations

in this structure worsens the separation obtained in the pure silica structure. On the contrary, the presence of sodium cations in BRE-type structures improves the adsorption selectivity compared with the pure silica structure. As shown in Figure 5, in this case the selectivity improves almost three times, and its absolute value increases even more at low temperatures. Therefore, the presence of sodium cations in BRE enhances the adsorption of carbon monoxide and worsens the adsorption of oxygen (Figure S7 of the Supporting Information).

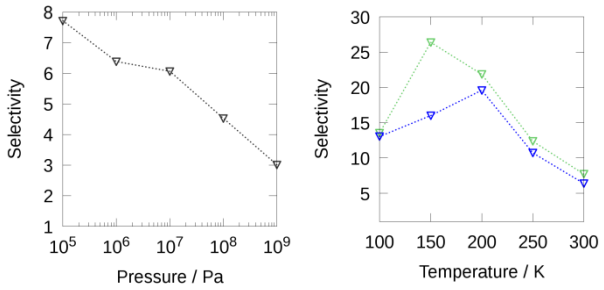

Figure 5. Adsorption selectivity of carbon monoxide over oxygen in BRE zeolite with 4 Na^+/Al pairs per unit cell as a function of pressure at 298 K (left) and as a function of temperature (right) at 10^5 Pa (green) and 10^6 Pa (blue). Isotherms to calculate selectivity come from molecular simulations.

Using both zeolite capacity and adsorption selectivity, we can provide different separation schemes that are depicted in Figure 6. At operating conditions of 300 K and 10^5-10^6 Pa the most efficient separation scheme using the screened zeolites consists in employing FAU for carbon dioxide removal followed by using BRE for the separation of carbon monoxide from oxygen. BRE containing aluminum atoms and sodium cations preferentially adsorbs carbon monoxide, letting oxygen pass through. These results could be even improved by working at lower temperatures than 300 K. On the contrary, to capture oxygen while carbon monoxide flows through can be achieved by using pure silica MTW zeolite, but it would be necessary to relax the operating conditions by increasing pressure and/or decreasing temperatures.

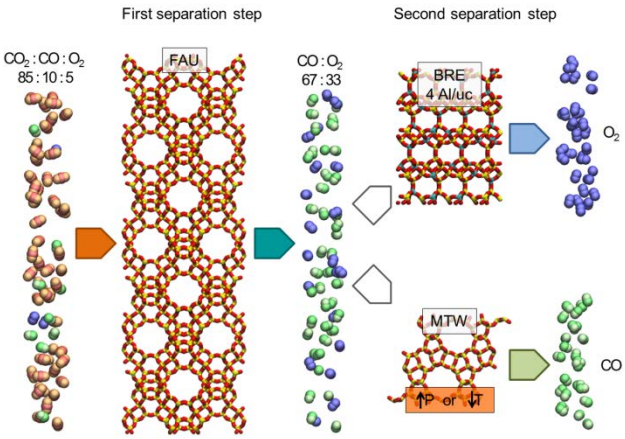

Figure 6. Separation scheme for the mixture CO_2 (85%), CO (10%) and O_2 (5%) using zeolites. Two options are available for the second separation step.

To verify the capabilities of the selected adsorbents in the desired separations at operating conditions, PSA simulations were performed for the removal of CO_2 from a mixture of CO_2 (85%), CO (10%) and O_2 (5%) using FAU zeolite as adsorbent, and the concentration of CO in the resulting light product (containing CO and O_2) using BRE zeolite with 4 Al/uc. Model parameters and operating conditions used in the simulations are shown in Table 3. For the first separation, a typical PSA cycle for hydrogen purification is considered,[29] which is called PSA cycle I from now on. For the second separation, a modification of the first cycle, including a rinse step to increase the concentration of CO in the heavy product[30] is considered, which is called PSA cycle II. Bed length and cycle time are also taken from Tomita *et al.*[29] A scheme, time schedule and pressure history of these cycles is given in Figure S8 in Supporting Information. Details about the working of these cycles are available elsewhere.[30]

Table 3. Model parameters and operating conditions in PSA simulations.

PSA cycle	I	II
Adsorbent	FAU	BRE

Feed composition, $CO_2/CO/O_2$, %v/v	85/10/5	0/65.7/34.3
Temperature, K	300	300
P_{HIGH}, P_{LOW}, bar	2, 0.1	2, 0.1
Bed length, m	1	1
Cycle time, min	8	8
Bed porosity	0.4	0.4
[a]Extracrystalline porosity	0.3	0.3
[b]Particle density, kg m^{-3}	940	1395
Particle radius, m	$7 \cdot 10^{-4}$	$7 \cdot 10^{-4}$
[c]Molecular diffusivity, 10^{-6} m^2 s^{-1}	8.4/8.5/8.6	-/10.1/10.1
Tortuosity	3	3
[c]μ, Pa s	$1.5 \cdot 10^{-5}$	$1.9 \cdot 10^{-5}$
[d]Adsorbent heat capacity, J kg^{-1} K^{-1}	1000	1000
[e]Isosteric heats, $CO_2/CO/O_2$, kJ mol^{-1}	17.3/9.99/9.31	-/28.8/21

[a] Taking a typical zeolitic pellet extracrystalline porosity from Tomita *et al.* [29]

[b] Calculated as crystal density*(1-extracrystalline porosity)

[c] Calculated with AspenPlus

[d] Jiang *et al.* 2017 [31]

[e] Average values calculated with Van't Hoff equation between zero loading and the loading at feed conditions

The multicomponent adsorption isotherms for the PSA simulations are obtained by applying the IAST method to the pure component isotherms. A comparison between the pure component fitted isotherms and molecular simulation data is shown in Figure S9. The resulting Langmuir parameters are shown in Table S2.

PSA cycle I is designed to meet the two following specifications: (i) CO_2 concentration in the light product (L) below 0.5 % v/v, and (ii) CO recovery in the light product above 85%. The feed gas velocity in the adsorption (ADS) step (u_F), the high pressure of the cycle (P_{HIGH}), and the final pressure of the provide purge (P_{PP}) step are considered to carry out a parametric study to measure their influence on the CO_2 concentration and the CO recovery in the light product. The CO_2 productivity in the heavy product (H) is also calculated to evaluate the process throughput. The results of the parametric study (contained in Table S3 in Supporting Information) shows that an increase in P_{HIGH} from 1 to 2 bar allows reaching high purity of light product and high CO recovery simultaneously. The separation performance improves if P_{PP} is increased from 0.9 to 1.0 bar. Increasing the feed gas velocity results on the one hand in lower product purity, because the adsorption front of CO_2 advances more along the bed in the ADS step, but on the other hand in higher recovery, because the bed has a higher loading of CO_2 during the regeneration and therefore a lower loss of light compounds in the heavy product. Designing the PSA cycle I with P_{HIGH} = 2 bar, P_{PP} = 1 bar, and u_F = 0.0064 m s^{-1} leads to the highest CO_2 productivity (0.1 kg kg^{-1} h^{-1}) and CO recovery (87.6%) for the runs fulfilling the purity specification. The resulting heavy product has the following composition: CO_2 (98.1%), CO (1.4%), O_2 (0.5%). This stream can be recycled to the plasma reactor to avoid CO losses in PSA cycle I and to reuse the CO_2 removed.

From Figure 7, it is clear that concentration of CO_2 is very low in the final part of the column when ending the ADS step, and there is a high concentration of CO and O_2 in the light product. Concurrently, the concentration of CO_2 at the end of regeneration (end of RP step) is very high. The temperature profiles show that the bed heats up notably as the CO_2 adsorption front

advances along the bed because of its high concentration in the feed, whereas it gets cooled during the regeneration due to desorption.

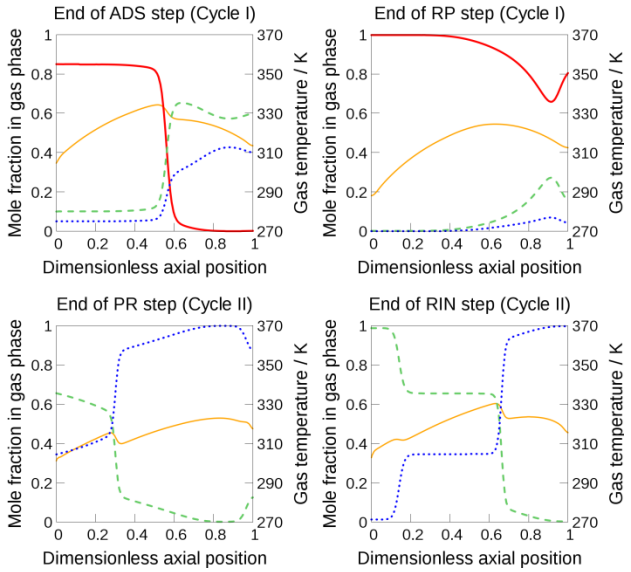

Figure 7. Top: Spatial profiles of composition and temperature at the end of ADS step (left) and at the end of RP step (right) in PSA cycle I. Bottom: Spatial profiles of composition and temperature at the end of PR step (left) and at the end of RIN step (right) in PSA cycle II. CO_2 plotted as solid red line, CO as dashed green line, O_2 as dotted blue line, and temperature as solid orange line.

The light product of PSA cycle I is then introduced as feed stream in PSA cycle II at the same pressure (2 bar). To simplify the design, the presence of CO_2 in this stream (below 0.5%) is neglected. On this basis, the composition of the feed mixture for PSA cycle II is CO (65.67%), O_2 (34.33%). The design specifications for this cycle are CO purity and recovery in the heavy product above 98%. After performing the same parametric analysis as for the previous cycle, it was found that the design specifications can be achieved with a P_{PP} = 0.8 bar, and a feed gas velocity of the ADS and rinse (RIN) steps of 0.022 m s^{-1}. Results at the onset of the light product production (end of PR step) and at the end of the light product production (end of the

RIN step) in PSA cycle II, shown in Figure 7, provide CO in the heavy product at a 98.73% purity with a 98.04% CO recovery, along with a productivity of 0.0575 kg CO kg^{-1} h^{-1}. Also, the O_2 purity in the light product is 96.3%, with an O_2 recovery of 97.6% and a productivity of 0.0342 kg O_2 kg^{-1} h^{-1}. The movement of the CO profile between the end of PR and RIN steps is indicative of the gradual loading of the bed with CO while releasing a light product with low CO concentration. The bed inlet reaches a very high concentration of CO due to the introduction of heavy product in the RIN step. This loading is recovered as high purity CO in the heavy product at the regeneration step. The good performance of this separation ultimately stems from the high selectivity of BRE zeolite towards CO in CO/O_2 mixtures, combined with the high linearity of the isotherms. Considering the whole industrial process, our results show that the desired separations can be carried out efficiently by PSA using the adsorbents we propose.

4. CONCLUSIONS

Molecular simulation in combination with Ideal Adsorption Solution Theory allows zeolite screening for the separation at mild operating conditions of a mixture of gases from carbon dioxide dissociation. Based on our screening, we suggest the use of FAU for removing CO_2 and BRE at 4 Al/uc to capture CO as the optimal zeolite framework combination for this separation. Conditions for a PSA process were optimized to enable an efficient separation. In the first PSA cycle (CO_2 removal), we recommend a high pressure of 2 bar, final pressure of the PP step of 1.0 bar, and feed gas velocity of 0.0064 m s^{-1}. The composition of the heavy product extracted would thus be 98.1% CO_2, 1.4% CO, and 0.5% O_2. This stream could then be recycled to the plasma reactor to avoid CO losses and to reuse the CO_2 removed. The second PSA cycle coupled to the first should set the final pressure of the PP step to 0.8 bar, and feed gas velocities of the ADS and RIN steps to 0.022 m s^{-1}. This yields 98.04% CO recovery at 98.73% purity with a productivity

of 0.0575 kg CO kg^{-1} h^{-1}. As for O_2, a 97.6% recovery at 96.3% purity is calculated with a productivity of 0.0342 kg O_2 kg^{-1} h^{-1}. It is worth noting that both FAU and BRE zeolites are already commercially available and the suggested process improvement could be straightforwardly implemented by the industry. The idea of separation mechanisms based on adsorption with zeolites is also transferable to other separations of industrial interest like olefin/paraffin separation in the European Petrochemical Industry. Market penetration of this technology in this area (ethane/ethylene, propane/propylene, etc.) would bring about substantial reductions in energy consumption, paving the way for the development of a long-term research strategy.

ASSOCIATED CONTENT

Supporting Information. Supplementary figures of adsorption isotherms, selectivity, and main structures, data of specific surface area, effective pore and selectivity for zeolites in screening, data and figures of the Langmuir fit for PSA cycles, and table of effect of the gas velocity in PSA cycle I.

AUTHOR INFORMATION

Corresponding Author

* E-mail: scalero@upo.es

ACKNOWLEDGMENT

This work is supported by the European Research Council through an ERC Starting Grant (ERC2011-StG-279520-RASPA and the Spanish Ministerio de Economía y Competitividad

(CTP2016-80206-P). I. Matito-Martos and S. R. G. Balestra thank Spanish Ministerio de Economía y Competitividad for their predoctoral fellowships.

REFERENCES

1. Jackson, R. B.; Canadell, J. G.; Le Quere, C.; Andrew, R. M.; Korsbakken, J. I.; Peters, G. P.; Nakicenovic, N., Reaching Peak Emissions. *Nat. Clim. Change* **2016,** *6* (1), 7-10.
2. Le Quéré, C.; Andrew, R. M.; Canadell, J. G.; Sitch, S.; Korsbakken, J. I.; Peters, G. P.; Manning, A. C.; Boden, T. A.; Tans, P. P.; Houghton, R. A.; Keeling, R. F.; Alin, S.; Andrews, O. D.; Anthoni, P.; Barbero, L.; Bopp, L.; Chevallier, F.; Chini, L. P.; Ciais, P.; Currie, K.; Delire, C.; Doney, S. C.; Friedlingstein, P.; Gkritzalis, T.; Harris, I.; Hauck, J.; Haverd, V.; Hoppema, M.; Klein Goldewijk, K.; Jain, A. K.; Kato, E.; Körtzinger, A.; Landschützer, P.; Lefèvre, N.; Lenton, A.; Lienert, S.; Lombardozzi, D.; Melton, J. R.; Metzl, N.; Millero, F.; Monteiro, P. M. S.; Munro, D. R.; Nabel, J. E. M. S.; Nakaoka, S.-i.; amp; apos; Brien, K.; Olsen, A.; Omar, A. M.; Ono, T.; Pierrot, D.; Poulter, B.; Rödenbeck, C.; Salisbury, J.; Schuster, U.; Schwinger, J.; Séférian, R.; Skjelvan, I.; Stocker, B. D.; Sutton, A. J.; Takahashi, T.; Tian, H.; Tilbrook, B.; van der Laan-Luijkx, I. T.; van der Werf, G. R.; Viovy, N.; Walker, A. P.; Wiltshire, A. J.; Zaehle, S., Global Carbon Budget 2016. *Earth System Science Data* **2016,** *8* (2), 605-649.
3. Lebouvier, A.; Iwarere, S. A.; d'Argenlieu, P.; Ramjugernath, D.; Fulcheri, L., Assessment of Carbon Dioxide Dissociation as a New Route for Syngas Production: A Comparative Review and Potential of Plasma-Based Technologies. *Energy Fuels* **2013,** *27* (5), 2712-2722.
4. Van Rooij, G.; van den Bekerom, D.; den Harder, N.; Minea, T.; Berden, G.; Bongers, W.; Engeln, R.; Graswinckel, M.; Zoethout, E.; van de Sanden, M., Taming Microwave Plasma to Beat Thermodynamics in CO2 Dissociation. *Faraday Discuss.* **2015,** *183*, 233-248.
5. Brehmer, F.; Welzel, S.; van de Sanden, M. C. M.; Engeln, R., CO and Byproduct Formation During CO2 Reduction in Dielectric Barrier Discharges. *J. Appl. Phys.* **2014,** *116* (12), 123303.
6. Fridman, A., *Plasma Chemistry*. Cambridge university press: 2008.
7. Krishna, R.; van Baten, J. M., In Silico Screening of Zeolite Membranes for CO2 Capture. *J. Membr. Sci.* **2010,** *360* (1-2), 323-333.
8. Krishna, R.; van Baten, J. M., Using Molecular Simulations for Screening of Zeolites for Separation of CO2/CH4 Mixtures. *Chem. Eng. J.* **2007,** *133* (1-3), 121-131.
9. Peng, X.; Cao, D., Computational Screening of Porous Carbons, Zeolites, and Metal Organic Frameworks for Desulfurization and Decarburization of Biogas, Natural Gas, and Flue Gas. *Aiche J.* **2013,** *59* (8), 2928-2942.
10. Lin, L. C.; Berger, A. H.; Martin, R. L.; Kim, J.; Swisher, J. A.; Jariwala, K.; Rycroft, C. H.; Bhown, A. S.; Deem, M. W.; Haranczyk, M.; Smit, B., In Silico Screening of Carbon-Capture Materials. *Nat. Mater.* **2012,** *11* (7), 633-641.
11. Braun, E.; Zurhelle, A. F.; Thijssen, W.; Schnell, S. K.; Lin, L.-C.; Kim, J.; Thompson, J. A.; Smit, B., High-Throughput Computational Screening of Nanoporous Adsorbents for CO2 Capture from Natural Gas. *Mol. Syst. Des. Eng.* **2016,** *1* (2), 175-188.

12. Matito-Martos, I.; Martin-Calvo, A.; Gutierrez-Sevillano, J. J.; Haranczyk, M.; Doblare, M.; Parra, J. B.; Ania, C. O.; Calero, S., Zeolite Screening for the Separation of Gas Mixtures Containing SO2, CO2 and CO. *Phys. Chem. Chem. Phys.* **2014,** *16* (37), 19884-19893.
13. Jeong, W.; Kim, J., Understanding the Mechanisms of CO2 Adsorption Enhancement in Pure Silica Zeolites under Humid Conditions. *J. Phys. Chem. C* **2016,** *120* (41), 23500-23510.
14. Bongers, W.; Bouwmeester, H.; Wolf, B.; Peeters, F.; Welzel, S.; van den Bekerom, D.; den Harder, N.; Goede, A.; Graswinckel, M.; Groen, P. W., Plasma-Driven Dissociation of CO2 for Fuel Synthesis. *Plasma Process. Polym.* **2017,** *14* (6).
15. Baerlocher, C.; McCusker, L. B. Database of Zeolite Structures. http://www.iza-structure.org/databases/.
16. Myers, A.; Prausnitz, J. M., Thermodynamics of Mixed-Gas Adsorption. *Aiche J.* **1965,** *11* (1), 121-127.
17. Dubbeldam, D.; Calero, S.; Ellis, D. E.; Snurr, R. Q., Raspa: Molecular Simulation Software for Adsorption and Diffusion in Flexible Nanoporous Materials. *Mol. Simul.* **2016,** *42* (2), 81-101.
18. Garcia-Sanchez, A.; Ania, C. O.; Parra, J. B.; Dubbeldam, D.; Vlugt, T. J. H.; Krishna, R.; Calero, S., Transferable Force Field for Carbon Dioxide Adsorption in Zeolites. *J. Phys. Chem. C* **2009,** *113* (20), 8814-8820.
19. Martin-Calvo, A.; Lahoz-Martin, F. D.; Calero, S., Understanding Carbon Monoxide Capture Using Metal–Organic Frameworks. *J. Phys. Chem. C* **2012,** *116* (11), 6655-6663.
20. Martin-Calvo, A.; Garcia-Perez, E.; Garcia-Sanchez, A.; Bueno-Perez, R.; Hamad, S.; Calero, S., Effect of Air Humidity on the Removal of Carbon Tetrachloride from Air Using Cu-BTC Metal-Organic Framework. *Phys. Chem. Chem. Phys.* **2011,** *13* (23), 11165-11174.
21. Martin-Calvo, A.; Gutierrez-Sevillano, J. J.; Parra, J. B.; Ania, C. O.; Calero, S., Transferable Force Fields for Adsorption of Small Gases in Zeolites. *Phys. Chem. Chem. Phys.* **2015,** *17* (37), 24048-24055.
22. Myers, A., Activity Coefficients of Mixtures Adsorbed on Heterogeneous Surfaces. *Aiche J.* **1983,** *29* (4), 691-693.
23. Rodríguez-Gómez Balestra, S.; Bueno-Perez, R.; Calero, S. Gaiast *Zenodo* [Online], 2016.
24. Delgado, J. A.; Águeda, V. I.; Uguina, M. A.; Brea, P.; Grande, C. A., Comparison and Evaluation of Agglomerated Mofs in Biohydrogen Purification by Means of Pressure Swing Adsorption (PSA). *Chem. Eng. J.* **2017,** *326*, 117-129.
25. Vemula, R. R.; Sircar, S., Comparative Performance of an Adiabatic and a Nonadiabatic PSA Process for Bulk Gas Separation—a Numerical Simulation. *Aiche J.* **2017,** *63* (9), 4066-4078.
26. Krishna, R.; Smit, B.; Calero, S., Entropy Effects During Sorption of Alkanes in Zeolites. *Chem. Soc. Rev.* **2002,** *31* (3), 185-194.
27. Löwenstein, W.; Lowenstein, M., The Distribution of Aluminum in the Tetrahedra of Silicates and Aluminates. *Am. Mineral.* **1954,** *39*, 92-96.
28. Dempsey, E., Molecular Sieves. *Society of Chemical Industry, London* **1968,** *293*.
29. Tomita, T.; Sakamoto, T.; Ohkamo, U.; Suzuki, M. In *The Effects of Variables in Fourbed Pressure Swing Adsorption for Hydrogen Purification*, Proceedings of the Second Engineering Foundation Conference on Fundamentals of Adsorption, Liapis, AI (ed), Engineering Foundation, Nueva York, 1987.

30. Delgado, J. A.; Agueda, V. I.; Uguina, M. A.; Sotelo, J. L.; Brea, P., Hydrogen Recovery from Off-Gases with Nitrogen-Rich Impurity by Pressure Swing Adsorption Using CaX and 5A Zeolites. *Adsorption* **2015,** *21* (1-2), 107-123.
31. Jiang, Y.; Ling, J.; Xiao, P.; He, Y.; Zhao, Q.; Chu, Z.; Liu, Y.; Li, Z.; Webley, P. A., Simultaneous Biogas Purification and CO2 Capture by Vacuum Swing Adsorption Using Zeolite Nausy. *Chem. Eng. J.* **2017,** *334*, 2593-2602.

TABLE OF CONTENTS